

PAPER • OPEN ACCESS

Accurate green water loads calculation using naval hydro pack

To cite this article: H Jasak *et al* 2017 *IOP Conf. Ser.: Mater. Sci. Eng.* **276** 012011

View the [article online](#) for updates and enhancements.

Related content

- [Application of foam-extend on turbulent fluid-structure interaction](#)
K Rege and B H Hjertager
- [Design of a New Water Load for S-band 750 kW Continuous Wave High Power Klystron Used in EAST Tokamak](#)
Liu Liang, Liu Fukun, Shan Jiafang et al.
- [Steady and unsteady numerical simulations of the flow in the Tokke Francis turbine model, at three operating conditions](#)
Lucien Stoessel and Håkan Nilsson

Accurate green water loads calculation using naval hydro pack

H Jasak*, **I Gatin¹**, and **V Vukčević²**

Faculty of Mechanical Engineering and Naval Architecture, University of Zagreb, Croatia

*Contact author: hrvoje.jasak@fsb.hr; ¹inno.gatin@fsb.hr; ²vuko.vukcevic@fsb.hr

Abstract. An extensive verification and validation of Finite Volume based CFD software Naval Hydro based on foam-extend is presented in this paper for green water loads. Two-phase numerical model with advanced methods for treating the free surface is employed. Pressure loads on horizontal deck of Floating Production Storage and Offloading vessel (FPSO) model are compared to experimental results from [1] for three incident regular waves. Pressure peaks and integrals of pressure in time are measured on ten different locations on deck for each case. Pressure peaks and integrals are evaluated as average values among the measured incident wave periods, where periodic uncertainty is assessed for both numerical and experimental results. Spatial and temporal discretization refinement study is performed providing numerical discretization uncertainties.

1. Introduction

Green water loads are of great importance when it comes to designing offshore objects due to their exposure to adverse weather conditions. Predicting green water loads accurately is a challenging task due to the nonlinearity of the flow on deck, causing engineers to turn towards more advanced numerical methods. Finite Volume (FV) based Computational Fluid Dynamics (CFD) methods are getting more attention for green water loads prediction, however the confidence among engineers is insufficient at this point due to the lack of verification and validation in the literature.

Temarel et al. [2] concluded that computational and experimental methods lack the maturity for green water load prediction, indicating that further research is needed on the topic. Even though there is a number of publications dealing with numerical methods for green water loads assessment, only a few compare the results with experiments. Greco et al. [3] performed wave load calculations on a patrol ship using CFD, comparing the results to experiments. Joga et al. [4] compared two CFD codes and experimental results for water ingress during green water events. Silva et al. [5] performed simulations of FPSO exposed to beam and quartering waves, where green water loads on deck structure is compared to experimental data. There are more publications dealing with green water loads, however few compare pressure loads with experiments, and even fewer show verification on green water cases.

This paper offers an extensive verification and validation for green water pressure loads of the Naval Hydro software pack, based on foam—extend, the open—source CFD software. FV method with collocated grid arrangement is used, where Volume of Fluid (VOF) method is used for interface



capturing, with geometric advection method called isoAdvector [6]. Ghost Fluid Method (GFM) is used for treating the kinematic and dynamic free surface boundary conditions at the interface [7]. A fixed FPSO model is used with a breakwater on deck, encountered by regular head waves. Three different waves are simulated, while the results are validated against experimental data published by Lee et al. [1]. Verification is performed using four refinement levels where spatial and temporal resolution is varied simultaneously [8], providing detailed numerical uncertainty assessment.

The paper is organized as follows. First, a brief overview of the numerical model is introduced, followed by the simulation set-up. Next, verification is shown with numerical uncertainties for each wave case, followed by result comparison. Finally, a short conclusion is given.

2. Numerical model

An incompressible, two—phase, viscous and turbulent fluid is modelled using the conservation of mass and momentum equations:

$$\nabla \cdot \mathbf{u} = 0, \quad (1)$$

$$\frac{\partial \mathbf{u}}{\partial t} + \nabla \cdot (\mathbf{u}\mathbf{u}) - \nabla \cdot \left(\nu \nabla \mathbf{u} \right) = -\frac{1}{\rho} \nabla p_d, \quad (2)$$

where \mathbf{u} stands for the velocity field, ν is the effective kinematic viscosity, comprising fluid kinematic viscosity and turbulent eddy viscosity, ρ is fluid density, while p_d stands for dynamic pressure, calculated as $p_d = p - \rho \mathbf{g} \cdot \mathbf{x}$, where p stands for total pressure, \mathbf{g} is gravitational constant, and \mathbf{x} is the position vector. Hence, the term denotes the hydrostatic pressure. Here, the free surface boundary conditions are discretized using Ghost Fluid Method [7], which imposes a physical jump of dynamic pressure and density field across the free surface. The method alleviates spurious air velocities from which two—phase FV codes often suffer. Apart from the above equations, a fraction field α transport equation is used to advect the interface:

$$\frac{\partial \alpha}{\partial t} + \nabla \cdot (\alpha \mathbf{u}) = 0. \quad (3)$$

Equation (3) is not discretized in conventional FV manner, instead a geometric method called isoAdvector is used to reconstruct the iso—surface representing the interface, which is then used to assess temporal and spatial integrals over cell—faces exactly. The reader is referred to [6] for more information on the isoAdvector method.

Implicit relaxation zones [9] are used to impose regular waves in the computational domain, and to damp diffracted waves towards the end of the domain by forcing them to the incident wave solution.

3. Simulation set up

Simulation set up is performed to comply exactly to the experimental measurements from [1], where three bow shapes are tested with nine regular incident waves each. In this paper, one bow shape is considered (RECT0) with three incident waves, with parameters shown in Table 1. For wave initialisation a nonlinear stream function wave model is used [10]. In the experiments, pressure is measured on ten locations on the horizontal deck. Figure 1 shows the geometry of the FPSO model used in the experiment where the positions of pressure gauges are also indicated.

Table 1. Incident wave parameters.

Wave ID	λ (m)	a (cm)	ka
1	2.25	6.750	0.188
2	3.00	6.000	0.126
3	3.00	7.500	0.157

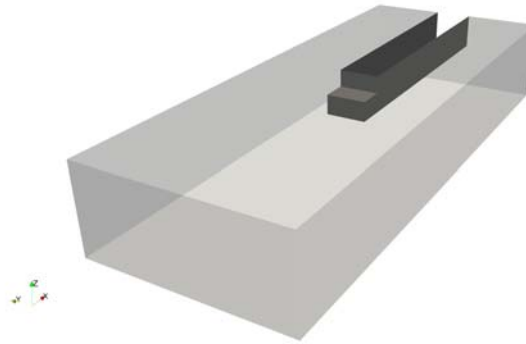


Figure 2. CFD computational domain.

Table 2. Number of cells in individual computational grids.

Wave ID	Grid 1	Grid 2	Grid 3	Grid 4
1	276 699	518 476	1 077 515	2 181 103
2	291 546	546 952	1 140 179	2 299 683
3	319 035	603 876	1 236 052	2 509 667

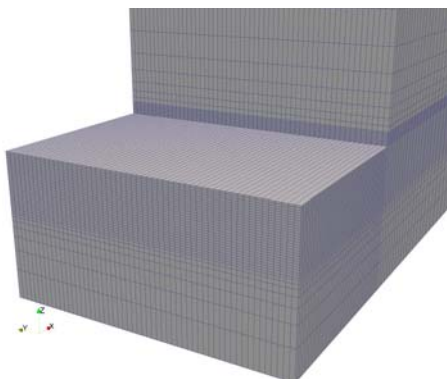


Figure 3. Discretized surface of the FSPO model for wave 2, Grid 1.

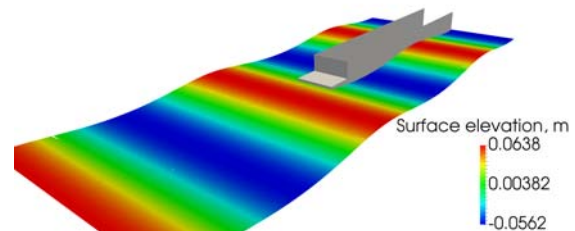


Figure 4. Initial condition for wave 2 simulation.

4. Verification

Numerical discretization uncertainties are calculated using the least squared method proposed by Eça and Hoekstra [8], where four discretization levels are needed. Instead of pressure values, total vertical pressure force on the horizontal deck is used for verification, since unlike pressure, it represents a smooth function in time. On the other hand, it is a spatial integral of pressure, and hence the calculated uncertainties are related to pressure in individual points. Figure 5 shows the time signal of vertical force acting on the deck during the simulation for wave 3. For each refinement level, the average force peak F_{max} , and average force integral in time over one wave period I , are calculated as:

$$F_{max} = \frac{\sum_{i=1}^{N_C} F_{i,max}}{N_C}, \quad (4)$$

$$I = \frac{\sum_{i=1}^{N_C} \int_0^T F_i(t) dt}{N_C}, \quad (5)$$

Where N_C represents the number of simulated periods, $F_{i,max}$ is the maximum force in the i -th period, and T is the wave period. These items are used to calculate numerical uncertainties which comprise periodic uncertainty between simulated wave periods, and numerical discretization uncertainty.

Numerical discretization uncertainties for each wave case are shown in Table 3, where $F_{0,max}$ and I_0 stand for the extrapolated theoretical exact solutions of force peak and force integral, respectively. They are obtained using the discretization refinement study [8]. $U_{CD,F}$ and $U_{CD,I}$ are discretization uncertainties of F_{max} and I , respectively. The uncertainties range from 2.2 to 20.7 percent, indicating the unsteady and violent nature of green water impact. It will be shown below that these uncertainties compare to experimental uncertainties.

Figure 6 shows the green sea event from wave 2 case simulation. The wave spills onto deck from the front and the sides, forming a circular water front. The water front converges towards the centreline as it approaches the breakwater, causing water impact and run-up. Next, the water column formed at the breakwater collapses, forming a rebound wave propagating towards the deck edges, and interacting with the subsequent incoming wave.

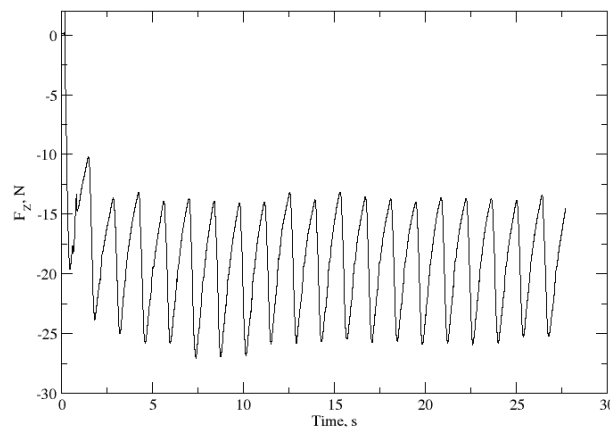
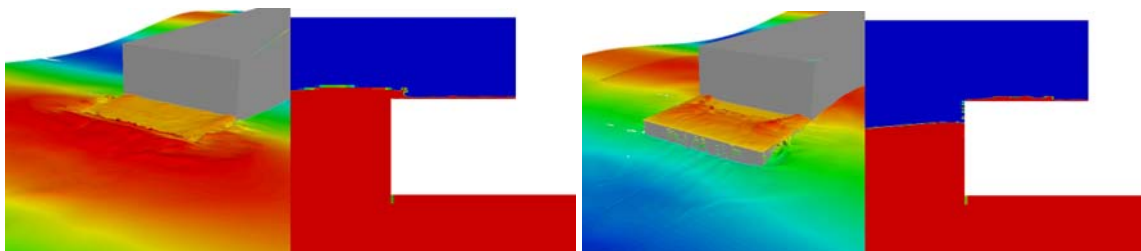


Figure 5. Vertical force measured at the deck for wave 3.

Table 3. Numerical discretization uncertainties.

Wave ID	$F_{0,max}$, N	$U_{CD,F}$, %	I_0 , Ns	$U_{CD,I}$, %
1	62.25	5.3	59.45	8.5
2	39.56	12.7	42.21	20.7
3	61.09	2.2	61.03	4.4



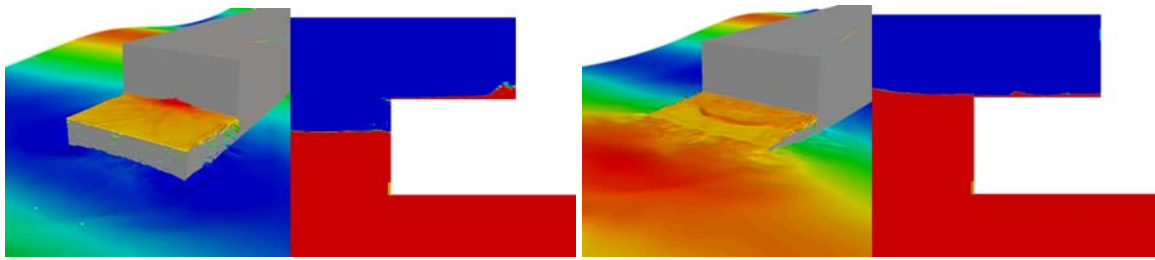


Figure 6. Sequential screen shots from wave 2 simulation on grid 3.

5. Validation

The simulation results are validated against experimental data from [1]. Pressure peaks p_{max} , and integrals in time P are compared to experimental values, calculated as:

$$p_{max} = \frac{\sum_{i=1}^{N_C} p_{i,max}}{N_C}, \tag{6}$$

$$P = \frac{\sum_{i=1}^{N_C} \int_0^T p_i(t) dt}{N_C}, \tag{7}$$

where $p_{i,max}$ denotes maximum pressure measured during one wave period.

Result comparison for all wave cases for pressure peaks measured at different pressure gauges is shown in Figure 7, Figure 8 and Figure 9. The error bars represent numerical and experimental uncertainties. Numerical uncertainties comprise periodic and discretization uncertainties, while experimental uncertainties arise from periodic and measuring uncertainties.

For wave 1 (Figure 7), trend and values agree well, where for only two out of ten gauges the uncertainty intervals do not overlap, while the uncertainties are comparable between CFD and the experiment (EFD). For wave 2 (Figure 8), the numerical uncertainties are larger than experimental, mainly due to large discretization uncertainties, Table 3. Nonetheless, values correspond well with the experimental results, where seven out of ten pressure gauges exhibit overlapping uncertainty intervals. Good agreement is observed for wave 3 as well on Figure 9, where the trend is well captured and the values being very close. Numerical uncertainties are generally smaller than experimental, except for pressure gauge 7 and 8, where the largest pressure loads occur. Overall, the agreement between experimental and computational results is acceptable.

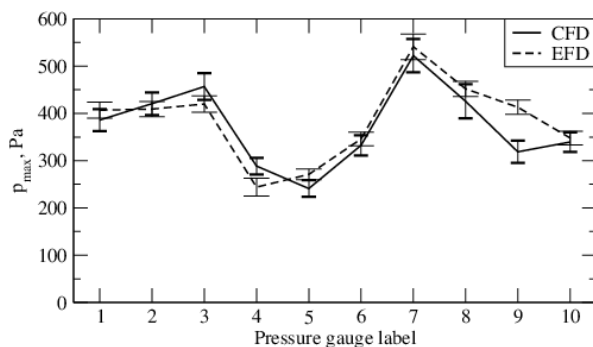


Figure 7. Pressure peak comparison for wave 1.

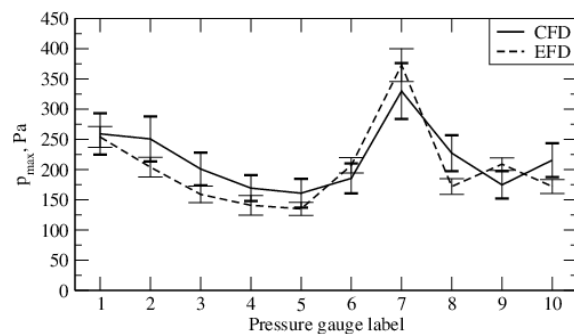


Figure 8. Pressure peak comparison for wave 2.

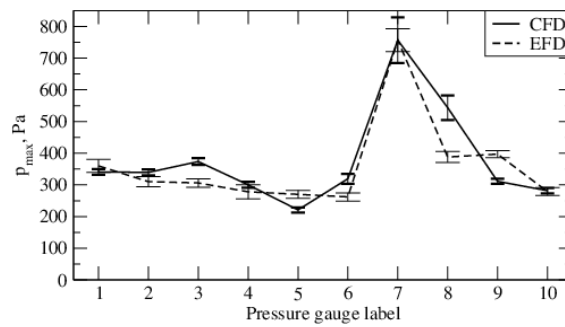


Figure 9. Pressure peak comparison for wave 3.

Comparison of pressure integrals in time is shown on Figure 10, Figure 11 and Figure 12. Numerical uncertainties of pressure integral for wave 1, Figure 10, are larger than experimental, however they remain within acceptable range. Trend and values correspond well, where numerical results mostly underestimate the experimental measurements. Same as for pressure peaks, wave 2, shown on Figure 11, exhibits larger numerical uncertainties with respect to two other wave cases. The values are well predicted for most gauges, with gauge 5 and 8 being an exception. For wave 3, pressure integrals comparison shown in Figure 12 exhibit small numerical uncertainties and good agreement with the experiment with overlap of uncertainty intervals, where pressure gauges 7 and 9 show larger discrepancies comparing to the remaining pressure gauges.

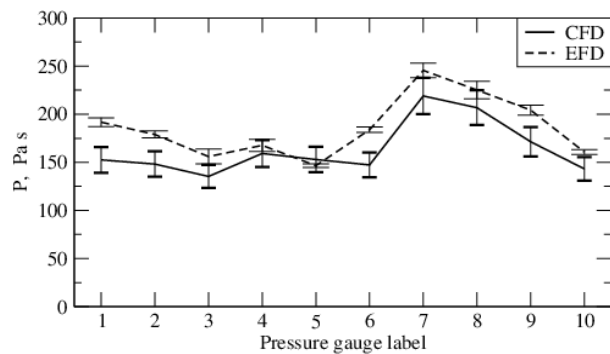


Figure 10. Comparison of pressure integral in time for wave 1.

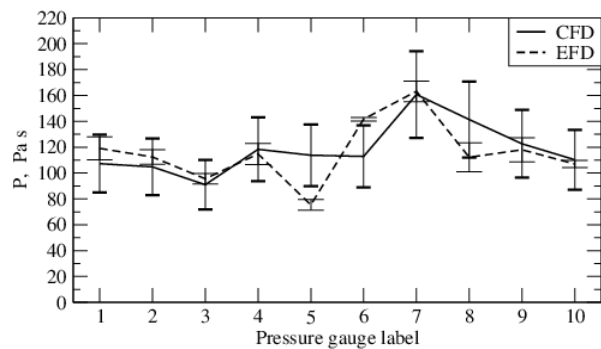


Figure 11. Comparison of pressure integral in time for wave 2.

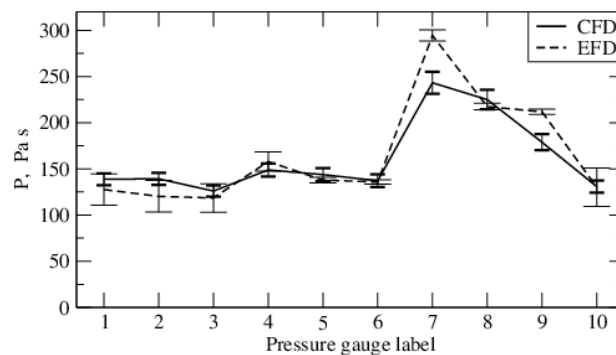


Figure 12. Comparison of pressure integral in time for wave 3.

Comparison between numerical and experimental results show that accurate prediction of green water pressure loads can be obtained at horizontal deck. The differences between the results often fall within the uncertainty range, while the trends over different gauges show good agreement.

6. Conclusion

Verification and validation of Naval Hydro software pack for green water pressure loads are presented in this paper. Fixed model of a simplified FPSO vessel is considered, encountered by three different regular waves causing green water events.

Detailed verification using four spatial and temporal refinement levels is performed in order to determine computational uncertainties. Acceptable uncertainties are obtained ranging from 2 to 20 percent, which are comparable to experimental uncertainties.

The results are validated against experimental data, where pressure peaks and time integrals are compared. Good agreement is achieved for all wave cases for values and trends, where only a few pressure gauges showed larger discrepancies.

This paper presents a step further towards gaining confidence in CFD for prediction of free surface impact loads. In future research, green water loads on vertical breakwater will be considered as well, since the designing of the same poses a challenge from structural load point of view.

Acknowledgement

This research was sponsored by Bureau Veritas under the administration of Dr. Šime Malenica.

References

- [1] Lee H H, Lim H J and Rhee S H 2012 Experimental investigation of green water on deck for a CFD validation database *Ocean Eng.*, **42** pp. 47–60.
- [2] Temarel P, Bai W, Bruns A, Derbanne Q, Dessi D, Dhavalikar S, Fonseca N, Fukasawa T, Gu X, Nestegård A, Papanikolaou A, Parunov J, Song K H and Wang S 2016 Prediction of wave-induced loads on ships: Progress and challenges *Ocean Eng.* **119** pp. 274–308.
- [3] Greco M, Bouscasse B, and Lugni C 2012 3-D seakeeping analysis with water on deck and slamming. Part 2: Experiments and physical investigation *J. Fluids Struct.* **33** pp. 127–47.
- [4] Joga R, Saripilli J, Dhavalikar S, and Kar A 2014 Numerical simulations to compute rate of water ingress into open holds due to green waters *In Proc. of the 24th Int. Offshore and Polar Eng. Conf. ISOPE (Busan)*
- [5] Silva D F C, Esperança P T T, and Coutinho A L G A 2017 Green water loads on FPSOs exposed to beam and quartering seas, Part II: CFD simulations *Ocean Eng.* **140** pp. 434–52.
- [6] Roenby J, Bredmose H, and Jasak H A 2016 Computational Method for Sharp Interface Advection *arXiv* p. 1601.05392.
- [7] Vukčević V, Jasak H, and Gatin I 2017 Implementation of the Ghost Fluid Method for free surface flows in polyhedral Finite Volume framework *Comput. Fluids* **153** pp. 1–19.
- [8] Eça L and Hoekstra M 2014 A procedure for the estimation of the numerical uncertainty of CFD calculations based on grid refinement studies *J. Comput. Phys.* **262** pp. 104–30
- [9] Jasak H, Vukčević V, and Gatin I 2015 Numerical Simulation of Wave Loads on Static Offshore Structures *In CFD for Wind and Tidal Offshore Turbines* pp. 95–105.
- [10] Rienecker M M and Fenton J D 1981 A Fourier approximation method for steady water waves *J. Fluid Mech.* **104** pp. 119–37
- [11] Eça L, Hoekstra M, Vaz G, Koop A, Pereira F, Abreu H *NPARC Alliance CFD Verification and Validation Web Site*,
- [12] Roache P J, Stern F, Wilson R V, Coleman H W, and Paterson E G 2016 Code Verification of Unsteady Flow Solvers with the Method of the Manufactured Solutions,” *Int. J. Offshore Polar Eng.* **29(1)** pp. 123–60